<Ogirinal>Tensile Shear Creep Test of Steel-Balsa-Steel Sandwich Panel as Floor Deck (I) : Stress Distribution and Deformation of Specimen

REZENDE, Maria Teresa R.; SASAKI, Hikaru; YANG, Ping

REZENDE, Maria Teresa R. ...[et al]. <Ogirinal>Tensile Shear Creep Test of Steel-Balsa-Steel Sandwich Panel as Floor Deck (I) : Stress Distribution and Deformation of Specimen. Wood research : bulletin of the Wood Research Institute Kyoto University 1987, 74: 12-22

Original

Tensile Shear Creep Test of Steel-Balsa-Steel Sandwich Panel as Floor Deck (I)

Stress Distribution and Deformation of Specimen*1

Maria Teresa R. REZENDE*2, Hikaru SASAKI*3
and Ping YANG*3

(Received September 1, 1987)

Abstract——Stress analysis by finite element method of tensile shear test specimens of steel-balsa-steel sandwich panel for creep test was made statically. The stress distribution of five different shapes of sandwich panel specimens, two of them in accordance with ASTM-C-273, were analysed through the calculation of normal stress (σ_Y), maximum principal stress (σ_1), shear stress (τ_{XY}) and principal shear stress (τ_{max}). The presence of stress singularities at the reentrant corners made by specimen and loading plates suggests fracture occurance in balsa core near the corner. Stress intensity factors (K_A) in balsa core near the corner were calculated under assumption of similarity with that in homogeneous body. The results obtained were as follows: 1) σ_Y, σ_1 and τ_{max} of balsa core concentrated near the reentrant corners, and τ_{XY} distribution was uniform throughout the balsa core, 2) Comparing K_A of various specimens it was suggested that the estimated fracture load on specimens shaped within the range specified by ASTM standard (length l/thickness $t \geqq 12$) did not vary. Fracture load of specimens with $l/t=8.2$, 6.3 and 4.2 were lower than those of the standard specimens. Therefore, the standard shape will be utilized in the further investigation: tensile shear creep test of sandwich panel as floor deck (II).

1. Introduction

Sandwich construction consists of three laminations of material bonded together. The outer two laminations, or facings, usually determine the elastic and strength properties of the construction; and the central lamination, or core, serve to separate the facings and to restrain them from becoming elastically unstable. Thus the facings are usually made of strong, stiff materials and the cores of light materials having only suffeciently great elastic and strength properties to

---

*1 A part of this paper was presented at the 37th Annual Meeting of the Japan Wood Research Society at Kyoto, April 1987.

*2 National Institute of Metrology, Standardization and Industrial Quality-SAS Qd. 2 lote 2/5 9-andar-70.070-Brasilia, DF-Brazil, as research fellow at Wood Research Institute, Kyoto University, Uji, Kyoto 611 Japan.

*3 Wood Research Institute, Kyoto University, Uji, Kyoto 611 Japan.

accomplish their purpose¹⁾. Therefore, sandwich construction is stiff and strong in comparison to its weight and useful for aircraft or other carriage as floor material, wall panels and so forth.

A number of evaluations of mechanical properties of sandwich have been made¹⁾. However, much of the testing has been limited to some statical properties; and the published reports have not generally included information about shear creep strength and deformation of core material. Due to the duration of load tensile creep testing is expensive and time consuming²⁾.

Though ASTM Standard specifies the test specimen to determine shear properties of sandwich construction, it is necessary to verify whether the specimen shape is proper in stress distribution or not.

The primary objectives of these series of study is to develop a simple shear creep test machine, and to test the efficacy of the machine. A secondary objective is to determine the correct shape of specimn to be utilized in these tests through the numerical analysis of finite element method.

In the present paper, stress distribution and deformation of five different shapes of specimen including two specimens according to ASTM were analysed in order to determine the specimen shape for the creep test.

2. Methd of Analysis

The computer program used in this study was of Finite Element Method for Plane Stress Analysis as an approximation of the problem. All computations were performed on a FACOM 380Q Computer of the Institute for Chemical Research, Kyoto University. The basic size of sandwich construction utilized in the analysis is in accordance with ASTM-C-273-61 (1970)³⁾, where a test specimen shall have a thickness equal to the thickness of the sandwich, a width not less than twice the thickness, and a length not less than 12 times the thickness.

In order to investigate the shape effect of specimen with steel-balsa-steel sandwich constructions, five different shapes of specimen were adopted. Those had the proportion of length (l)/thickness (t) as following:

$l/t = 15.6^*$, 12.0^*, 8.2, 6.3 and 4.2,

where, only the thickness of the balsa core were variable. The steel loading plates utilized in this analysis, due to the necessity to protecting the sandwich surface against undulation, had 250 × 50 × 10 mm in size. The test method adopted has been used generally as tensile shear test of sandwich construction (ASTM-C-

---

* These relations are in accordance with ASTM-C-273, where a length thickness ratio of 12:1 is prescribed as a minimum.

273). The loading applied was 1,300 kgf*, and the line of action of the direct tensile force passed through the diagonally opposite reentrant corners made by specimin and loading plates.

An example of the idealized specimen system with many imaginary finite elements, and boundary conditions for calculation are shown in Fig. 1. Total 465 nodes and 768 triangular elements were employed. The center of balsa core was fixed so as to adjust the loading direction to the line passed through the diagonal opposite reentrant corner of specimen. The load was applied on the various specimens with their respective positions which can be seen in the appended table of Fig. 1.

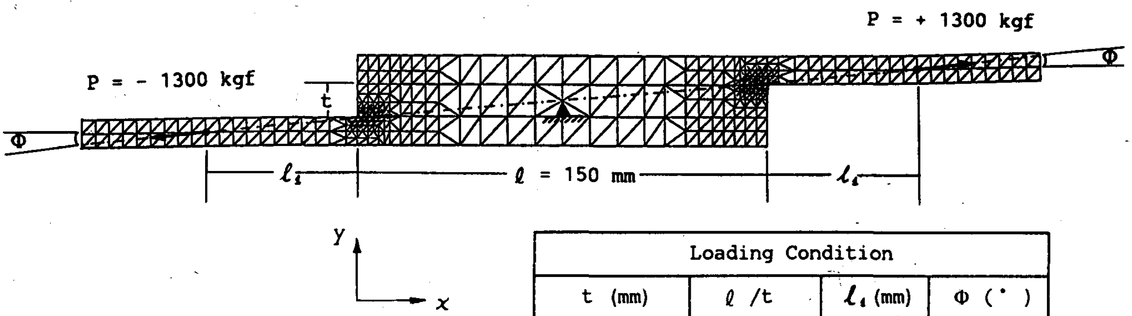

Loading Condition			
t (mm)	ℓ /t	ℓ_i (mm)	Φ (°)
9.63	15.6	65	4.9
12.50	12.0	55	5.1
18.25	8.2	50	6.2
24.00	6.3	35	10.3
35.50	4.2	25	14.1

t: Thickness of sandwich specimen.

Fig. 1. Idealization of specimen system and boundary conditions.

It was assumed here that the thickness of glue-lines were very thin, and also the adhesion between the balsa core and stainless steel facings, as well as the facings and loading plates were bonded rigidly. It means that either slip or movement was neglected at the interfaces. This is usually achieved, in practice, with nail-glued or press-glued4).

The elastic constants used in the calculation ae shown in Table 1. The data of E, μ and G were obtained by the average of species of balsa with different densities, as:

$$E_x = (E_R+E_T)/2,$$

$$E_y = E_L,$$

---

* The value has sometimes been adopted commercially as a minimum requirement (250 psi) for specimens with balsa core.

Table 1. Elastic constants of the steel and balsa used in the calculation

Material	Elastic constant*
Steel	Young's Modulus in x Direction E_x=0.21 × 10^5 kgf/mm^2 Young's Modulus in y Direction E_y=0.21 × 10^5 kgf/mm^2 Poisson's Ratio μ_{yx}=0.3 Modulus of Rigidity G_{xy}=0.81 × 10^4 kgf/mm^2
Balsa	E_x=0.142 × 10^2 kgf/mm^2 E_y=0.445 × 10^3 kgf/mm^2 μ_{yx}=0.36** G_{xy}=0.186 × 10^2 kgf/mm^2

* From R.F.S. Hearmon⁵⁾. ** From Wood Handbook⁶⁾.

$$\mu_{yx}=(\mu_{LR}+\mu_{LT})/2,$$
$$G_{xy}=(G_{LT}+G_{LR})/2,$$

Where, suffixes L, R and T mean longitudinal, radial and tangential axes directions of wood respectively.

3. Results and Discussions

Fig. 2 shows the displacements of each specimen analysed. For better visualization of the displacements, their values were magnified by 25. As the shape of specimens used in the present study and the force applied on them were diagonally symmetrical about the center point of the specimens, the displacements observed were also symmetrical with respect to the center point.

The stress distribution in balsa core was also diagonally symmetrical. The stress concentration took place near the reentrant corners between loading plates and specimen. This can be attributed to the bending occured at the loading plates, in spite of the fact that no conspicuous bending deformation have been produced as presented above. When the thickness of the loading plates increases the stress concentration of the reentrant corners of balsa core will decrease.

Table 2 shows the maximum values of stress (σ_X, σ_Y) and shear stress (τ_{XY}) of each specimen system. The maximum value of compressive stress (σ_X) occured in the loadig plates due to bending effect at the back sides of the reentrant corners, and the maximm value of tensile stress (σ_Y) was located on the stainless steel plate near the reentrant corners. The maximum value of shear stress (τ_{XY}) was observed on the loading plates, adjacent to the reentrant corners. Analysing only the portion of balsa core it was observed that the tensile stress (σ_Y) concentrated at the reentrant corners, while the shear stress (τ_{XY}) distribution was fairly uniform.

Table 3 shows the maximum values of principal stress (σ_1) and maximum

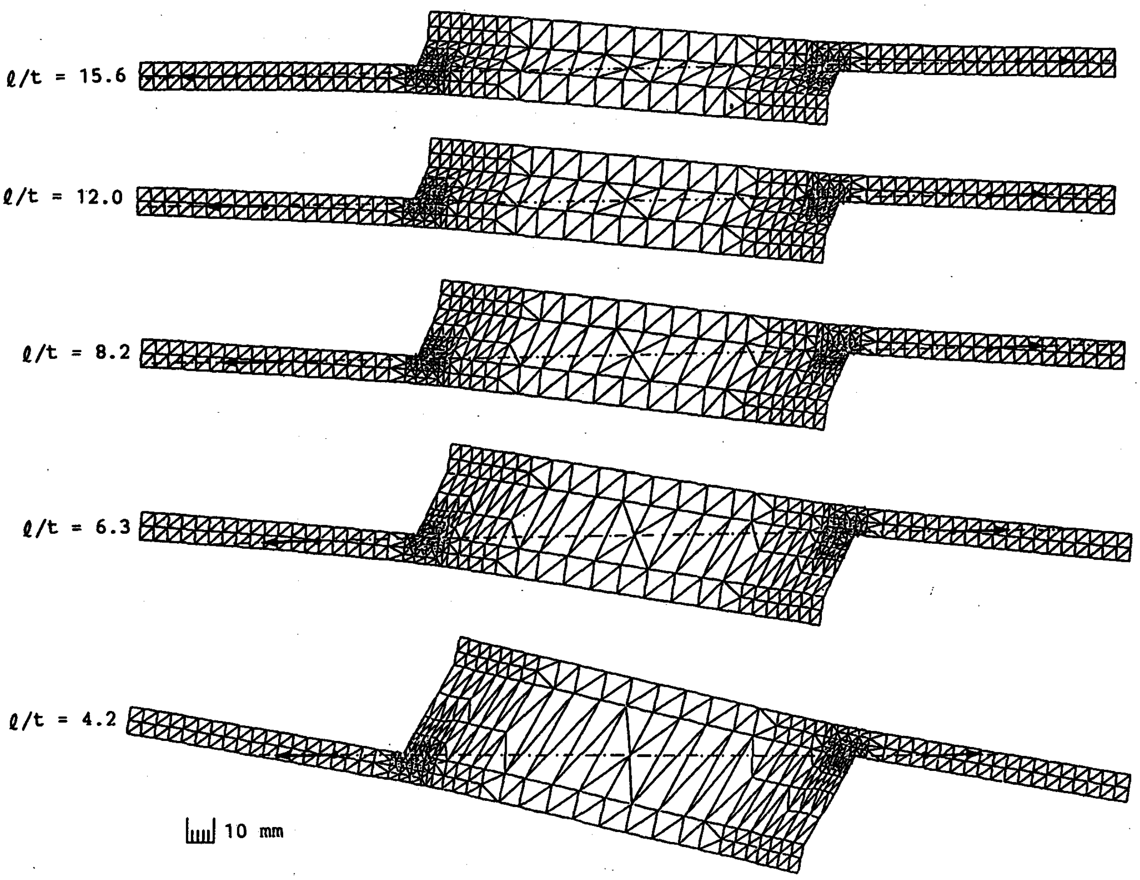

Fig. 2. Deformation of the specimen system. Values of displacement are expressed in magnification, ×25.

Table 2. Computed values of the maximum normal stress (σ_x, σ_y) and shear stress (τ_{xy}) of specimen

Specimen shape (l/t of sandwich)	Maximum normal stress (kgf/mm^2)		Maximum τ_{xy} (kgf/mm^2)
	Compression σ_x	Tension σ_y	
15.6	−1.01	+4.13	2.40
12.0	−0.88	+4.01	2.21
8.2	−1.01	+4.49	2.39
6.3	−1.21	+4.98	2.65
4.2	−0.95	+4.70	2.30

values of principal shear stress (τ_{max}) of the balsa core, in each specimen. All distribution of principal stress (σ_1) and principal shear stress (τ_{max}) of balsa core are shown in Fig. 3. The notation and sign convention which were used for principal stress (σ_1) and principal shear stress (τ_{max}) are indicated in the figure, and an angle of 45° from the arrow σ_1 to the arrow τ_{max} in counterclockwise is formed; also to express compression or tension values, the arrows are convergent

Table 3. Computed values of the maximum principal stress (σ_1) and shear stress ($\tau_{\max}$) of balsa core

Specimen shape (l/t of sandwich)	Maximum σ_1 (kgf/mm^2)	Maximum $\tau_{\max}$ (kgf/mm^2)	Element having maximum σ_1, $\tau_{\max}$*
15.6	1.62	0.82	267
12.0	1.73	0.87	267
8.2	2.08	1.04	267, 498
6.3	2.36	1.18	267
4.2	2.48	1.24	498

* Refer to figure 3 for the locations of the elements.

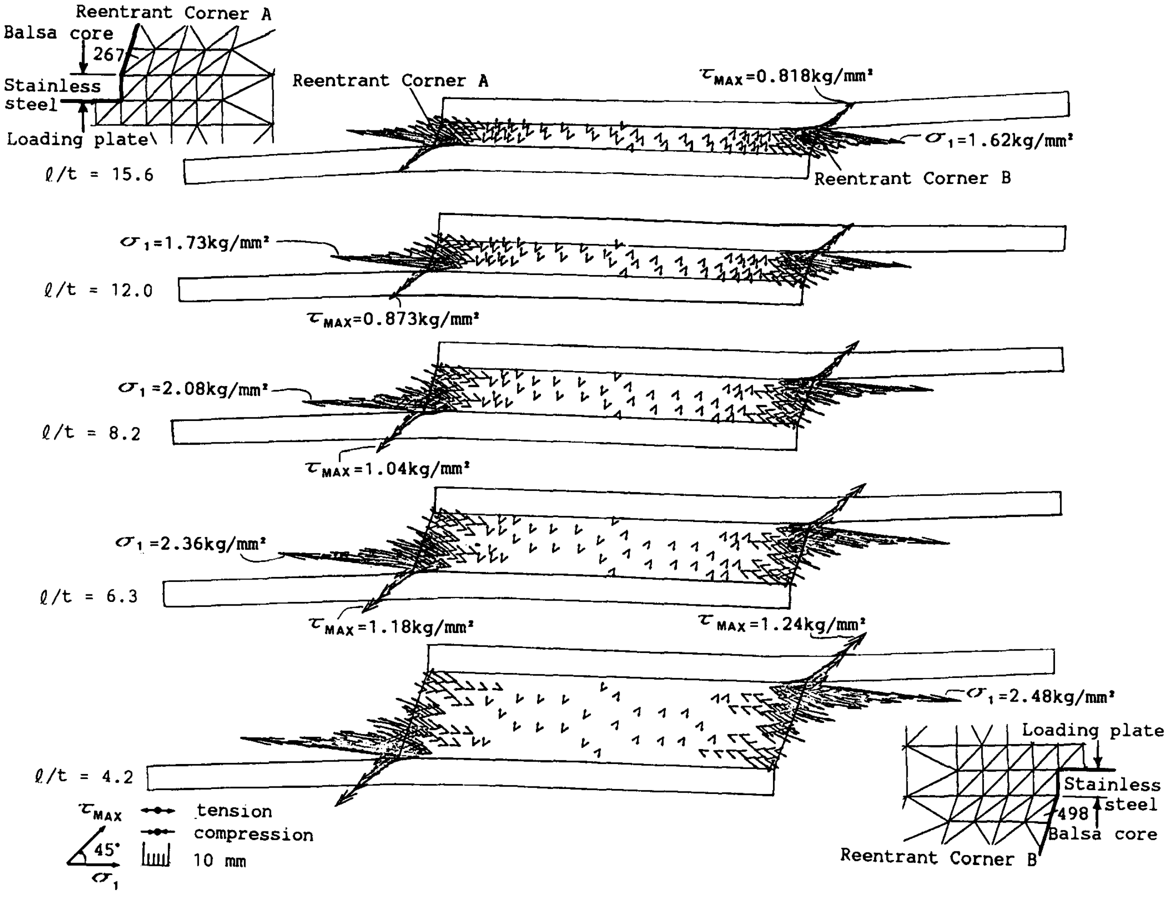

Fig. 3. Distribution of principal stress σ_1 and shear stress $\tau_{\max}$ in balsa core.

or divergent of the point correspondent to the weight centre of element, respectively. For the specimens utilized in this study the stress distribution were not uniform; the maximum principal stress (σ_1), principal shear stress ($\tau_{\max}$) and normal stress (σ_Y) of balsa core concentrated around the reentrant corners of the specimen system and fairly lower stress was observed at the centre of specimens. For shear stress (τ_{XY}) the distribution was fairly uniform throughout the balsa

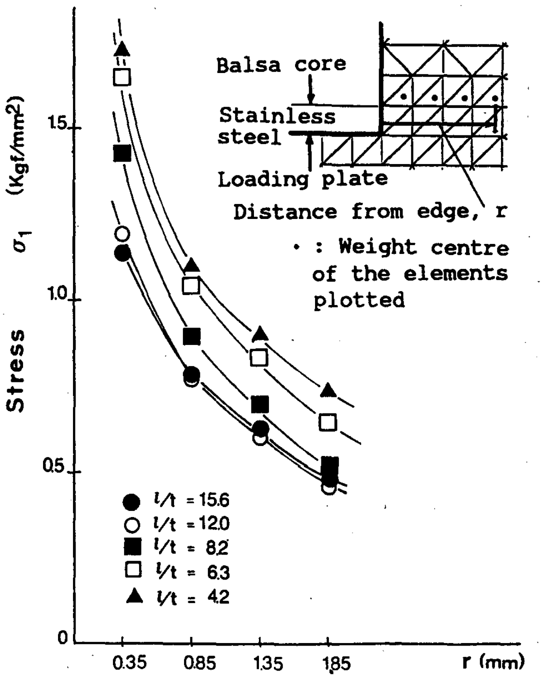

Fig. 4. Principal stress σ_1 distribution of balsa core elements near the reentrant corner of the specimen system.

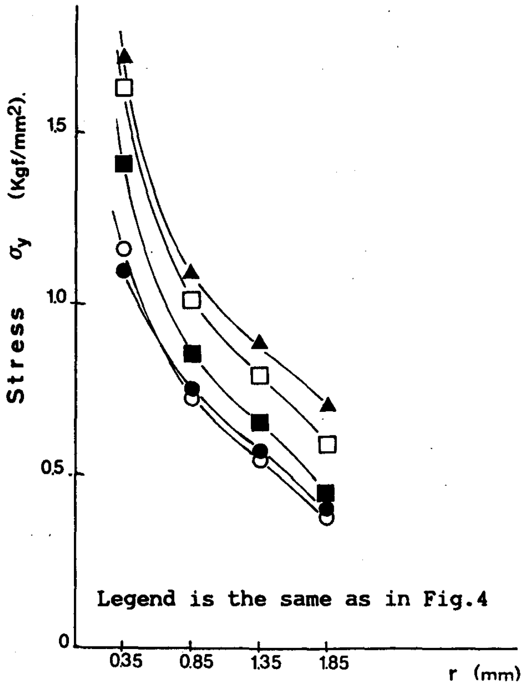

Fig. 5. Normal stress σ_y distribution of balsa core elements near the reentrant corner of the specimen system.

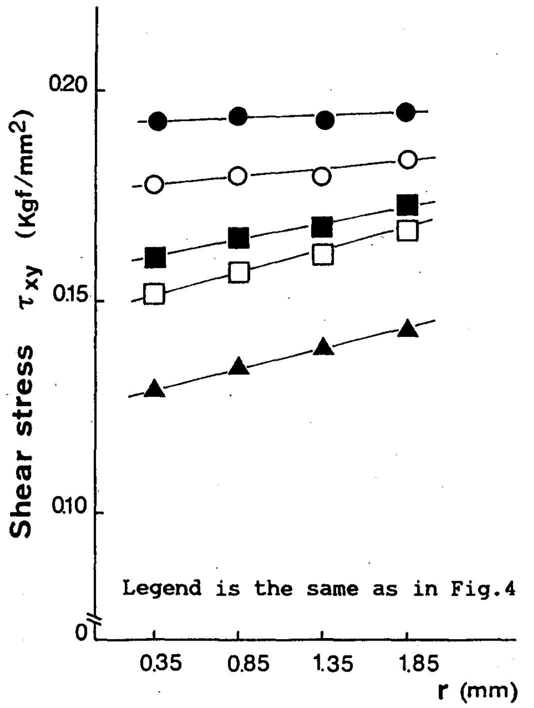

Fig. 6. Shear stress τ_{xy} distribution of balsa core elements near the reentrant corner of the specimen system.

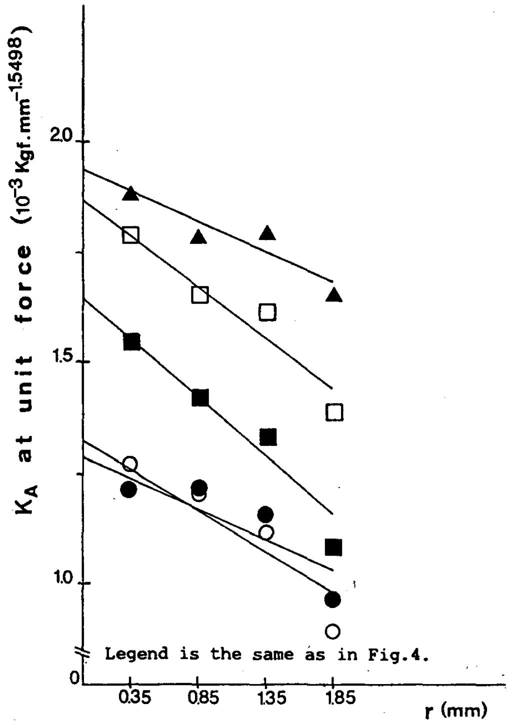

Fig. 7. Stress intensity factor K_A of balsa core elements near the reentrant corner of the specimen system.

core. Special elements near the stress concentration were taken to plot principal stress (σ_1) versus distance in x direction from the corner r, normal stress (σ_Y) versus r, and shear stress (τ_{XY}) versus r, as shown in Fig. 4, 5 and 6, respectively.

It was assumed in the present paper that failure would initiate near to the balsa part at the reentrant corner of the specimen system, and tensile stres (σ_Y) would play the most dominant role to the crack initiation. It was also assumed that the field of stress singularity near the reentrant corner in this steel-balsa composites would have some similarity in regard to the shape effect of the specimen system to that in homogeneous body. The stress σ_Y would be express as follows:

$$\sigma_Y = K_A/(2\pi r)^n$$

where, K_A is stress intensity factor for the stress singular point having a right angulr notch as defined by Leicester[7-11]. The value of n (=0.4502) was derived by Leicester[7-10] for wood with a right angular notch having an edge parallel to

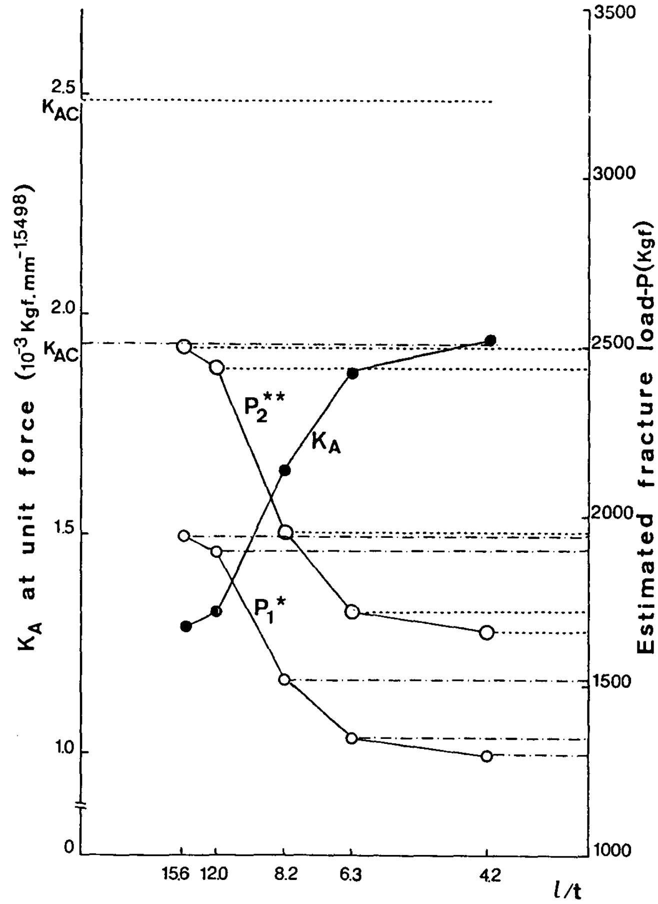

Fig. 8. Critical stress intensity factor K_{AC} and the estimated fracture load for different shapes of specimen.
* Calculated values for test condition 1 shown in Appendix.
** Calculated values for test condition 2 shown in Appendix.

the fiber direction. This equation was utilized to plot K_A at unit force versus distance from the edge r for each specimen, as shown in Fig. 7. As can be seen from the figure, when r decreases the stress intensity factor K_A insreases. Comparison between different shapes of specimens shows that for those with standard relation $l/t \geqq 12$ similar values of K_A are obtained, and for thicker specimen the K_A tends to increase with the thickness increasing.

If one utilizes experimental data of shear strength test (see Appendix) of specimen shape $l/t=12.0$, it is possible to obtain the critical stress intensity factor (K_{AC}) from the K_A per unit force at $r=0$ (Fig. 7) and to estimate fracture load for specimens with different shape as shown in Fig. 8. From these, it was observed that for experimental results of specimen tested at condition 1 (see Appendix) the estimated fracture load is lower than for specimen tested at condition 2. Also, as one can estimate fracture load for another shapes of specimens, the similar estimating method can be applied. Analysing the shape effect of the specimens it is possible to observe that for those with standard relation $l/t \geqq 12$ the estimated fracture load is higher than those without standard shape.

Conclusions

From numerical analysis it was observed, on the whole, that the stress concentration occured around the reentrant corners and the stresses were fairly lower at the centre of balsa core. Assuming that stress singularities occured at the end corners of balsa and comparing the stress intensity factors of various shape of specimens it was observed that in specimens with standard relation $l/t \geqq 12$ the estimated fracture loads are higher than those with l/t equal 8.2, 6.3 and 4.2.

Based on the results of theory and experiment, the standard ASTM specimn ($l/t \geqq 12$) was found suitable for tensile shear tests and this shape of specimen will be used in the report: Tensile shear creep test of steel-balsa-steel sandwich panel as floor deck (II)—Development of simple shear creep test machine.

Acknowledgments

The authors wish to thank the members of the Composite Wood Section, Wood Research Institute, Kyoto University for their help and suggestions. This study was supported in part by a Grant-in-Aid (60302082) from the Ministry of Education of Japan.

References

1) U.S. Dept. Air Force, Navy, Commerce. Sandwich construction for aircraft. Part II Materials properties and design criteria. ANC-23 Bull. (1955).
2) C.C. Gerhards and R.F. Pellerin: Effect of shock loading from series testing on tensile

strength of lumber and connector systems. Forest Prod. J., **34**(1), 38-43 (1984).
3) American Society for Testing and Materials. Standard methods of shear test in flatwise plane of flat sandwich constructions or sandwich cores. ASTM Designation C-273-61 (1970).
4) S.P. TAKINO: Numerical analysis of stress distribution of the actual size wood bearing wall in relation to the framing type. Wood Res. Inst. Bull., No. 64, 33-48 (1978).
5) R.F.S. HEARMON: The elasticity of wood and plywood. Dept. of Scientific and Industrial Research; Forest Products Research. Special Rept., No. 7, London (1948).
6) U.S. Dept. of Agriculture. Forest Products Laboratory. Wood Handbook (1955).
7) R.H. LEICESTER: The size effect of notches. Proceedings of the second Australasian Conference on the Mechanics of Structures and Materials (1969).
8) P.F. WALSH: Linear fracture mechanics in orthotropic materials. Eng. Fracture Mechanics **4**, 533 (1972).
9) P.F. WALSH: Stress intensity factors by a calibrated finite element method. ASCE Eng. Mech. J. Dec. (1972).
10) P.F. WALSH, R.H. LEICESTER and A. RYAN: The strength of glued lap joints in timber. Forest Prod. J. **23**(5), 30-33 (1973).
11) H. SASAKI: Fracture (ed. K. NAKATO: Mokuzai Kogaku, Yokendo (Tokyo)), 192-193 (1985).

Appendix

Tensile shear strength test of sandwich construction was made in accordance with ASTM-C-273[3]. Different specimen conditions were tested, and two of them were selected for this report. Condition 1 was the standard for the series of experiment and condition 2 was the best result obtained.

The core materials were end-grain balsa wood with 150×50×11.7 (fiber direction) mm in size, and their surfaces were prepared using 80 mesh sandpaper. Stainless steel plates previously back-primed with 150×50×0.4 mm in size were the sandwich faces.

Epoxy resin adhesive spreaded on core surface amounted 400 g/m^2 (type-Kanebo NSC: KBK-ER26, resin and KBK-ER13, hardner). For condition 1, the sandwich was pressed at 7 kg/cm^2 during 20 hours, and for condition 2 the pressure of 3 kg/cm^2 was applied.

Loading steel plates with 250×50×10 mm in size were attached to the sandwich faces second generation acrylic adhesive Diabond SG-11 formulated by Nogawa Chemical Co. Ltd. Load was applied through universal joints in a Olsen type 5 ton testing machine. Five replications were used for each condition, and the results are shown in Table 4.

Table 4. Experimental results

Condition	Maximum shear force (kgf)			
	Max.	Min.	Aver.	SD.
1	2, 020	1, 750	1, 896	103. 6
2	2, 560	2, 175	2, 439	154. 3